The use of microfluidics and dielectrophoresis for separation, concentration, and identification of bacteria

Cynthia Hanson, Michael Sieverts, Karen Tew,
Annelise Dykes, Michaela Salisbury, Elizabeth Vargis
Department of Biological Engineering, Utah State University
4105 Old Main Hill, Logan, UT, USA 84322

ABSTRACT

Traditional bacterial identification methods take one to two days to complete, relying on large bacteria colonies for visual identification. In order to decrease this analysis time in a cost-effective manner, a method to sort and concentrate bacteria based on the bacteria's characteristics itself is needed. One example of such a method is dielectrophoresis, which has been used by researchers to separate bacteria from sample debris and sort bacteria according to species. This work presents variations in which dielectrophoresis can be performed and their associated drawbacks and benefits specifically to bacterial identification. In addition, a potential microfluidic design will be discussed.

Keywords: Dielectophoresis, microfluidics, cell sorting, Raman spectroscopy, bacterial identification

1. INTRODUCTION

The standard method to identify bacteria is the use of an array agar media and associated antibiotics. Depending on bacterial growth among the array, the bacteria can be identified. This method is entirely dependent on the growth rate of the bacteria. Typically, bacteria will take one to two days to grow to colonies large enough for visual identification, while others may take weeks. For time sensitive illnesses, this lag in analysis time is unacceptable and has been the motivation for many researchers to find a faster methods to identify bacteria.

Common methods to decrease the analysis time of bacteria include techniques such as polymerase chain reaction (PCR) [1–5], Raman or infrared spectroscopy [6–8], fluorescent in situ hybridization (FISH) [9–11], and micro-array testing [12–16]. Raman spectroscopy has been used in our lab to spectrally distinguish between *Mycobacterium JLS*, *Mycobacterium KMS*, and *Mycobacterium MCS*. Spectra of these bacteria are shown in Figure 1. In lab, accuracy rates were as high as 96.7% using principal component analysis and linear discriminant analysis. Despite speed and accuracy of the most techniques presented in literature and from our lab, each method requires a pure sample or a means to label bacteria with fluorescent tags, antibiotics, or primers. A real life sample may be from blood, saliva, sputum, urine, etc. As such, samples must be pretreated prior to analysis to remove debris or separate other bacteria in the case of a sample containing more than one bacteria. The use of fluorescently marked antibodies increase costs and may result in wasted materials due to the broad range of bacteria strains that can be present in a sample. As such, label-free identification methods are appealing to cut costs and increase simplicity.

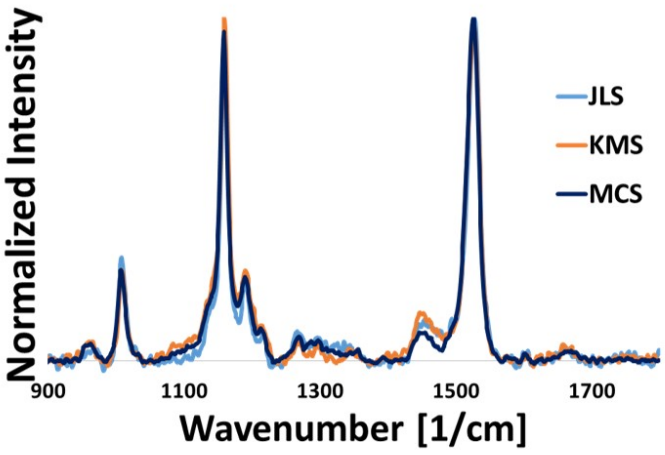

Figure 1. Baseline corrected, normalized spectra of *M. JLS*, *M. KMS*, and *M. MCS*.

One label-free method is dielectrophoresis (DEP). Dielectrophoresis is the use of non-uniform electric fields which causes motion in particles due to the electrical properties of the particle and surrounding fluid as well as the applied electric field. Dielectrophoresis is well suited for biological samples and has been used by many researchers for bacterial analysis such as discrimination between live and dead bacteria[17], isolation of specific strains of bacteria[18], and separating bacteria from sample debris[19].

Although dielectrophoresis was introduced in the early 1950s, its use in various research fields remained fairly dormant until the 1990s when techniques such as photolithography assisted in fabrication of minute structures like microfluidic devices. This advancement in fabrication techniques was crucial for DEP as it drastically dropped voltage requirements due to proximity of electrodes to cells within a sample, thus creating a much more realistic means for sample sorting. As a result, the use of DEP in microfluidic devices as well as the methods of implementation have significantly increased.

This article will briefly present the mathematics associated with dielectrophoresis and then present several different forms in which dielectrophoresis has been implemented. The benefits and drawbacks in accordance for bacterial analysis for each method will be discussed. In addition, a proposed form to carry out DEP will be presented and compared to the other methods.

2. DIELECTROPHORESIS

2.1 Theory of dielectrophoresis

Dielectrophoresis (DEP) was introduced by Pohl[20] in 1951. In Pohl's article, some mathematics to explain DEP were laid out. Pohl also referenced previous researcher which had witnessed DEP but could not explain it or mistakenly attributed it to electrophoresis. Although other researchers had witnessed the phenomenon, Pohl was first to associate a name to the occurrence.

The equation to express the DEP force on a spherical particle is

$$F_{DEP} = 2\pi\varepsilon_m r^3 Re[f_{CM}]\nabla|E_{rms}|^2 \quad (1)$$

where r is the radius of the particle, and E_{rms} is the root-mean-square of the electric field, ε is the permittivity with a subscript of m to indicate the media. Subscripts of p indicate particle. The real part of the Clausius-Mossotti factor is factor is expressed as

$$Re[f_{CM}] = \frac{\varepsilon_p^* - \varepsilon_m^*}{\varepsilon_p^* + 2\varepsilon_m^*} \tag{2}$$

where the asterisks indicate the complex permittivity. The complex permittivity is dependent on the conductivity (σ) and the frequency of the applied field (f) and is given by

$$\varepsilon^* = \varepsilon - \frac{j\sigma}{2\pi f} \tag{3}$$

where j is the square root of negative one. When the Clausius-Mossotti factor is positive, the DEP force will push the particle to a region with a strong electric field. This is referred to as positive DEP. In negative DEP, the Clausius-Mossotti factor is negative and the force pushes the particle to a region with a weak electric field. The point where the Clausius-Mossotti factor switches from positive to negative is referred to as the crossover frequency.

The homogeneity of the particle will influence the DEP force. The equations expressed previously are for homogeneous particles. For biological samples this is not the case as the electrical properties between the cytoplasm and the plasma membrane are different. For such situations, a single-shell model can be used where the plasma membrane is represented as a shell and the cytoplasm as the material inside the shell. Assuming this cytoplasm is homogenous, the complex permittivity of the shell-sphere can be express as

$$\varepsilon_{s-s}^* = \varepsilon_{mem}^* \frac{2\varepsilon_{mem}^* + \varepsilon_{cyto}^* - 2v(\varepsilon_{mem}^* - \varepsilon_{cyto}^*)}{2\varepsilon_{mem}^* + \varepsilon_{cyto}^* + v(\varepsilon_{mem}^* - \varepsilon_{cyto}^*)} \tag{4}$$

where ε_{mem}^* and ε_{cyto}^* are the complex electrical permittivity for the cell membrane and cytoplasm respectively and $v = (1 - d/R)^3$ with d being the membrane thickness and R the outer radius of the cell membrane. The complex permittivity for the shell-sphere can then replace ε_p^* in Equation 2. Although this model better matches biological cells, bacteria cells require yet another step as bacteria are composed of a cell wall, cell membrane, and cytoplasm (assuming homogeneity inside the cell membrane). In which case, a two-shell method must be incorporated, and thus the complex permittivity of a bacteria cell would be expressed as

$$\varepsilon_{cell}^* = \varepsilon_{wall}^* \frac{2\varepsilon_{wall}^* + \varepsilon_{s-s}^* - 2w(\varepsilon_{wall}^* - \varepsilon_{s-s}^*)}{2\varepsilon_{wall}^* + \varepsilon_{s-s}^* + w(\varepsilon_{wall}^* - \varepsilon_{s-s}^*)} \tag{5}$$

where $w = (1 - d_w/R_c)$ and the thickness of the cell wall and radius of the cell are d_w and R_c respectively. This expression for the complex permittivity of the cell can substitute ε_p^* in Equation 2 to calculate the Clausius-Mossotti factor for a two-shell spherical particle.

For more complex but realistic shapes such as a homogenous ellipsoid, Equation 2 changes to

$$Re[f_{CM}] = \frac{1}{3}\frac{(\varepsilon_p^* - \varepsilon_m^*)}{\varepsilon_m^* + A_i(\varepsilon_p^* - \varepsilon_m^*)} \tag{6}$$

where A_i is a component the depolarization factor which is along one of the axis (x, y, or z) of the ellipsoid. Assuming a prolate spheroid with the major axis on the x axis, the depolarization factor would be expressed as

$$A_x = \frac{1-e^2}{2e^3}\left[\log\left(\frac{1+e}{1-e}\right) - 2e\right] \tag{7}$$

where

$$e = \sqrt{1 - \left(\frac{b}{a}\right)^2} \tag{8}$$

and a is the major axis of the ellipsoid while b is the minor axis. To account for a double shell configuration, the expressions change. Using articles from Huang et al.[21,22] and Castellarnau et al.[23], the following equations were compiled. The effective dipole factor as a function of angular frequency, ω, for a single shell system is expressed as

$$X_{1,i}(\omega) = \frac{1}{3}\frac{(\varepsilon^*_{cyto}-\varepsilon^*_{mem})}{\varepsilon^*_{mem}+A_{1,i}(\varepsilon^*_{cyto}-\varepsilon^*_{mem})} \tag{9}$$

where

$$A_{1,x} = \frac{1-e_1^2}{2e_1^3}\left[\log\left(\frac{1+e_1}{1-e_1}\right) - 2e_1\right] \tag{10}$$

and e_1 is the same expression as in Equation 8. It should be noted that the following relationship exists due to rotational symmetry:

$$A_{1,z} = A_{1,y} = \frac{1-A_{1,x}}{2} \tag{11}$$

To account for the influence due to the cell wall, yet another layer must be added. The effective dipole moment is expressed as

$$X_{1,i}(\omega) = \frac{1}{3}\frac{(\varepsilon^*_{mem}-\varepsilon^*_{wall})+3X_{1,i}\rho_1[\varepsilon^*_{mem}+A_{2,i}(\varepsilon^*_{wall}-\varepsilon^*_{mem})]}{[\varepsilon^*_{wall}+A_{2,i}(\varepsilon^*_{mem}-\varepsilon^*_{wall})]+3X_{1,i}\rho_1 A_{2,i}(1-A_{2,i})(\varepsilon^*_{mem}-\varepsilon^*_{wall})} \tag{12}$$

where ρ_1 is the volume ratio expressed as

$$\rho_1 = \frac{a\cdot b^2}{(a+d_{mem})\cdot(b+d_{mem})^2} \tag{13}$$

and $d_{mem}$is the thickness of the membrane. The depolarization factor, $A_{2,i}$, remains the same as Equation 10 with the exception that all the subscripts change from 1 to 2. The eccentricity changes to

$$e_2 = \sqrt{1-\left(\frac{b+d_{mem}}{a+d_{mem}}\right)^2}. \tag{14}$$

The Clausius-Mossotti factor can then be expressed as

$$Re[f_{CM}]_i = \frac{1}{3}\frac{(\varepsilon^*_{wall}-\varepsilon^*_m)+3X_{2,i}\rho_2[\varepsilon^*_{wall}+A_{3,i}(\varepsilon^*_m-\varepsilon^*_{wall})]}{[\varepsilon^*_m+A_{2,i}(\varepsilon^*_{wall}-\varepsilon^*_m)]+3X_{2,i}\rho_2 A_{3,i}(1-A_{3,i})(\varepsilon^*_{wall}-\varepsilon^*_m)} \tag{15}$$

where

$$e_3 = \sqrt{1-\left(\frac{b+d_{mem}+d_{wall}}{a+d_{mem}+d_{wall}}\right)^2} \tag{16}$$

and

$$\rho_2 = \frac{(a+d_{mem})\cdot(b+d_{mem})^2}{(a+d_{mem}+d_{wall})\cdot(b+d_{mem}+d_{wall})^2}. \tag{17}$$

In Equations 16 and 17 $d_{wall}$is the thickness of the cell wall. To account for all axes, the Clausius-Mossotti factor is expressed as an average.

$$Re[f_{CM}] = \frac{1}{3}\sum_{i=x,y,z} Re[f_{CM}]_i \tag{18}$$

In our lab with *M. JLS*, *KMS*, and *MCS*, the bacteria have an ellipsoidal shape and therefore Equations 9-18 will be used to model DEP forces on the bacteria. In previous work done in our department, SEM and AFM images of each bacteria has been collected[24]. Using these images, average bacteria sizes have been determined. However, cell wall and membrane thicknesses have not been determined. Literature indicates a range of mycobacteria cell wall thicknesses from 8-26nm[25,26] depending on species and susceptibility. The dimensions measured from SEM and AFM images along with estimates from literature will be used in subsequent modeling studies in our lab.

3. DIELECTROPHORETIC DESIGN

3.1 Traditional dielectrophoresis

Initially, DEP was performed on microfluidic devices using metallic electrodes embedded within the sample chamber and thus created the electric field gradient. This arrangement was used by many researchers especially for bacterial separation and concentration[19,27,28]. However, the design had inherent problems such as electrode fouling, increased in sample temperature, and spatial limitations. Rise in sample temperatures are particular concern for biological samples as too high of temperatures can lead to cell death. The problem of spatial limitation refers to how close the cells must be to be influenced by the electric field, which is approximately 30 micrometers. Spatial problems can be partially addressed by patterning electrodes to the top and bottom of the sample chamber or along the full height of the channel. However, this does not completely resolve the problem as narrowing channels for proximity sake decreases throughput. Alternative designs such as insulator-based DEP (iDEP) and contactless DEP (cDEP) among others have been implemented and successfully overcome these spatial limitations while maintaining a high throughput.

3.2 Insulator-based dielectrophoresis

Insulator-based DEP (iDEP) incorporates the use of insulator structures within a microfluidic device to create electric field gradients as opposed to using the shape and configuration of metal electrodes to create the non-uniform electric field. In iDEP, electrodes are placed on opposite ends of a microfluidic device in direct contact with the sample solution. An array of insulator posts are placed in between the electrodes. This arrangement forces the electric field to move around the structures and creates a non-uniform electric field required for DEP.

When using iDEP, the electric field as well as the required voltage can be manipulated by altering size and shape of the insulator structures. This has been demonstrated in literature by observing the changes in electric field while using insulator posts in a variety of shapes (circles, diamonds, squares, etc.)[29,30] as well as spacing of posts in an array[31]. Using iDEP in an array, bacteria has been concentrated and separated from water[32] as well as from other bacteria in the same sample[33]. In addition, an iDEP array has been used to separate live and dead *E. coli*[17].

A variation of iDEP is gradient insulator dielectophoresis (g-iDEP), which incorporates not only an electric field gradient at the specific site but also throughout the channel. This is has been done by using a saw tooth pattern which gradually come closer together over the length of the microfluidic channel[34,35] as illustrated in Figure 2. Specific to bacterial studies, this method has been used as a means to separate serotypes of *E. coli*[18] and to separate *Staphyloccocus epidermidis* based on antibiotic susceptibility to gentamicin[36].

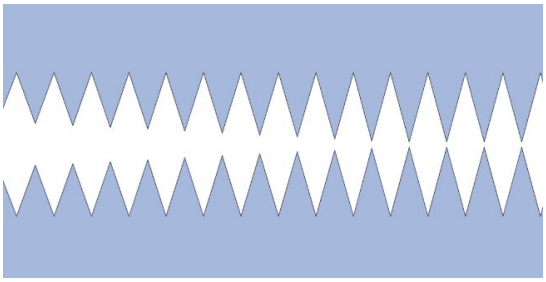

Figure 2: Illustration of gradient-iDEP device with a sawtooth pattern such that the pattern converges creating a gradient non-uniform electric field.

Insulator-based DEP has also been done in the form of partial obstruction of the microfluidic channel[37–39], examples of which are illustrated in Figure 3. Examples of using iDEP and partial obstruction for bacterial isolation include concentrating and separating *Bacillus subtilis* from a multicomponent mixture[38] and separating *E. coli* from blood cells[40].

Figure 3: Examples of iDEP devices with partial obstruction. Illustrations are of a side view were the sample indicated by the dark grey color moves from left to right.

3.3 Contactless dielectrophoresis

Contactless dielectrophoresis (cDEP) describes a DEP design where the electrodes have no direct contact with the sample chamber[41–44]. This can be done by forming three different chambers separated by an insulating material. One chamber is for the sample while the other two are for the electrodes. The non-uniform electric field is generated by either insulator structures within the sample chamber or simply the change in size and shape of the sample chamber. This method is highly dependent on the insulator material used and how thin of insulating layer can be made between the sample channel and the electrodes[43]. The design of cDEP avoids problems bubbles formation at electrodes, electrode fouling, and electrolysis. In addition, cDEP devices are quite simple to make once a master mold is created. After which, fabrication consists of simply casting PDMS on the mold and sealing the PDMS structure to a glass slide. The fabrication can be troublesome due to the requirement of such a thin membrane (~20 micrometers) between the sample channel and the electrode channels. The thinner membranes require less voltage but run the risk of dielectric breakdown during operation. Thinner membranes also increase the difficulty of forming a proper seal between the PDMS and the glass slide.

3.4 Carbon based electrode dielectrophoresis

In the past decade, the use of 3D carbon electrodes arrays for DEP-based separations has increased. This design incorporates structures similar to those related to iDEP with an array of posts within the sample. Unlike iDEP where the array is made of insulating material, the array in carbon electrode DEP are the electrodes themselves. This design allows for some advantages in lower applied voltages. An example of carbon based electrode DEP device for bacteria is the purification of *Mycobacterium smegmatis* to identify antibiotic susceptibility[45].

3.6 Comparison of designs

The previous list of DEP methods is not comprehensive. However, it does provide a reasonable base to assess general advantages and drawbacks for bacterial separation for future analysis. A more complete review of DEP methods including fabrication and functionality can be found in literature[46]. This article is concerned with development and functionality of DEP devices specifically for separation and concentration of bacteria for subsequent identification. As such, devices ideally avoid undesirable conditions for cells such as increased sample temperature and exposure to high voltages. At the same time, the device would need to be easily reproducible, durable during operation, and capable of exposing target particles to electric fields for effective sorting.

Devices which incorporate direct exposure of the sample to metallic electrodes such as traditional or iDEP approaches have the hardest time avoiding electrolysis and avoiding Joule heating. Electrolysis isn't as much as a problem with iDEP devices as the electrodes are far from the area in which DEP functions are carried out. However, electrolysis at the electrodes can create conditions such as a shift pH and associated aggregation of proteins which will influence DEP behavior[47]. Carbon based DEP still experience electrolysis, however these devices allow for lower voltage requirements as opposed to iDEP. Joule heating is also a concern particularly for iDEP devices as high voltages can increase sample temperature and rupture cells[48]. In contrast, cDEP deals with electrolysis and Joule heating much better as the sample channel has no contact with the electrodes.

For DEP to effectively sort a sample, the target particles must have adequate exposure to DEP forces. Devices which depend on the arrangement of metallic electrodes to create the electric field gradients are most hindered by this

requirement. As stated previously, particles must be within approximately 30 micrometers of the electrodes. This is especially problematic for planar electrodes. Researchers have worked around this problem by fabricating electrodes through electroplating. However, this drives up fabrication costs.

In terms of reproducibility and durability, cDEP arguably is most challenged by these aspects. The design of cDEP devices require an excellent seal between the elastomer and glass surface to avoid contamination between the electrode and sample channels. Providing a good seal between these two surfaces is complicated due to the thin membrane (approximately 20 micrometers) required. In addition, if the membrane is too thin, the device runs the risk of dielectric breakdown.

As demonstrated, each DEP method has advantages and drawbacks. Ideally, a device will incorporate the strengths of each design allowing for effective separation of target molecules regardless of position in the sample channel while avoiding risks of electrolysis. In addition, an ideal device would be durable and simple to produce.

4. PROPOSED DESIGN

The DEP methods presented previously in this paper used PDMS as a means to form the microfluidic channel when properly sealed to glass. The nature of PDMS lends these devices to be cheap and disposable. Although this can be a desirable characteristic, the use of PDMS or other elastomers come with inherent problems such as low stiffness making high aspect-ratio channels difficult to construct depending on the application and requirements. Ensuring a good seal between glass and PDMS may also proof problematic due to channel design. To avoid these problems, we propose forming a cDEP microfluidic device entirely of glass.

Several research groups have been striving to create robust, low-cost techniques to form glass microfluidic structures[49,50]. Companies have also demonstrated the ability and ease by which to form glass microfluidic devices with 20:1 etch rate of exposed to unexposed glass[51]. With these developments, producing a cDEP device with an adequately thin membrane offers advantages over the traditional form of fabrication with PDMS. Glass structures would be more resilient to higher voltages allowing for a wider range of operation before dielectric breakdown of the membrane. For PDMS membranes between 2-14 μm, the dielectric breakdown has been reported between 250-635 V/μm [52]. In contrast, alkali-free glass has a dielectric breakdown of 1000 V/μm[53] for thicknesses of 5-20 micrometers.

It is proposed to fabricate a cDEP microfluidic device solely out of glass to avoid issues associated with electrolysis experienced in other common forms of DEP, while capitalizing on the benefits of a reproducible and durable design. With a thin membrane composed of glass rather than PDMS, higher operating voltages can be applied without damaging the device. In addition, a glass microfluidic structure allows for reuse of the device even after autoclaving to remove any bacteria from previous samples.

REFERENCES

[1] Pechorsky, A., Nitzan, Y. & Lazarovitch, T., "Identification of pathogenic bacteria in blood cultures: Comparison between conventional and PCR methods," J. Microbiol. Methods 78(3), 325–330 (2009).

[2] Mirnejad, R., Mohamadi, M., Piranfar, V., Mortazavi, S. M. & Kachuei, R., "A duplex PCR for the rapid and simultaneous detection of Brucella spp. in human blood samples," Asian Pac. J. Trop. Med. 6(6), 453–456 (2013).

[3] Frickmann, H. et al., "Increased detection of invasive enteropathogenic bacteria in pre-incubated blood culture materials by real-time PCR in comparison with automated incubation in Sub-Saharan Africa," Scand. J. Infect. Dis. 45(8), 616–622 (2013).

[4] Teranishi, H. et al., "Detection of bacteria and fungi in blood of patients with febrile neutropenia by real-time PCR with universal primers and probes," J. Infect. Chemother. 21(3-4), 189–193 (2015).

[5] Zhou, L. & Pollard, A. J., "A fast and highly sensitive blood culture PCR method for clinical detection of Salmonella enterica serovar Typhi," Ann. Clin. Microbiol. Antimicrob. 9, 14 (2010).

[6] Maquelin, K. et al., "Prospective study of the performance of vibrational spectroscopies for rapid identification of bacterial and fungal pathogens recovered from blood cultures," J. Clin. Microbiol. 41(1), 324–329 (2003).

[7] Liu, T.-Y. et al., "Functionalized arrays of Raman-enhancing nanoparticles for capture and culture-free analysis of bacteria in human blood," Nat. Commun. 2, 538 (2011).

[8] Wang, H. et al., "Simultaneous capture, detection, and inactivation of bacteria as enabled by a surface-enhanced Raman scattering multifunctional chip," Angew. Chem.-Int. Ed. 54(17), 5132–5136 (2015).
[9] Kempf, V. A. J., Trebesius, K. & Autenrieth, I. B., "Fluorescent in situ hybridization allows rapid identification of microorganisms in blood cultures," J. Clin. Microbiol. 38(2), 830–838 (2000).
[10] Tajbakhsh, S., Gharibi, S., Zandi, K. & Yaghobi, R., "Use of a modified fluorescent in situ hybridization procedure to improve the identification of Streptococcus pneumoniae in blood cultures," Acta Microbiol. Immunol. Hung. 60(3), 303–311 (2013).
[11] Horvath, A., Kristof, K., Konkoly-Thege, M. & Nagy, K., "Rapid identification of pathogens in blood culture with fluorescent in situ hybridization (FISH)," Acta Microbiol. Immunol. Hung. 57(3), 225–234 (2010).
[12] Samuel, L. P. et al., "Evaluation of a microarray-based assay for rapid identification of gram-positive organisms and resistance markers in positive blood cultures," J. Clin. Microbiol. 51(4), 1188–1192 (2013).
[13] Kim, S. Y. et al., "Direct identification of Gram-positive bacteria and resistance determinants from blood cultures using a microarray-based nucleic acid assay: in-depth analysis of microarray data for undetermined results," Clin. Chem. Lab. Med. 53(7), 1013–1024 (2015).
[14] Buchan, B. W. et al., "Multiplex identification of gram-positive bacteria and resistance determinants directly from positive blood culture broths: Evaluation of an automated microarray-based nucleic acid test," Plos Med. 10(7), e1001478 (2013).
[15] Fishbain, J. T., Sinyavskiy, O., Riederer, K., Hujer, A. M. & Bonomo, R. A., "Detection of extended-spectrum beta-lactamase and Klebsiella pneumoniae Carbapenemase genes directly from blood cultures by use of a nucleic acid microarray," J. Clin. Microbiol. 50(9), 2901–2904 (2012).
[16] Shi, Y.-H. et al., "Detection of bacterial pathogens in aquaculture samples by DNA microarray analysis," Aquaculture 338, 29–35 (2012).
[17] Lapizco-Encinas, B. H., Simmons, B. A., Cummings, E. B. & Fintschenko, Y., "Dielectrophoretic concentration and separation of live and dead bacteria in an array of insulators," Anal. Chem. 76(6), 1571–1579 (2004).
[18] Jones, P. V., DeMichele, A. F., Kemp, L. & Hayes, M. A., "Differentiation of Escherichia coli serotypes using DC gradient insulator dielectrophoresis," Anal. Bioanal. Chem. 406(1), 183–192 (2014).
[19] Cheng, I.-F., Chang, H.-C., Hou, D. & Chang, H.-C., "An integrated dielectrophoretic chip for continuous bioparticle filtering, focusing, sorting, trapping, and detecting," Biomicrofluidics 1(2), 021503 (2007).
[20] Pohl, H. A., "The motion and precipitation of suspensoids in divergent electric fields," J. Appl. Phys. 22(7), 869–871 (1951).
[21] Huang, J. P., Yu, K. W., Lei, J. & Sun, H., "Spectral representation theory for dielectric behavior of nonspherical cell suspensions," Commun. Theor. Phys. 38(1), 113–120 (2002).
[22] Huang, J. P., Yu, K. W., Gu, G. Q. & Karttunen, M., "Electrorotation in graded colloidal suspensions," Phys. Rev. E 67(5), 051405 (2003).
[23] Castellarnau, M., Errachid, A., Madrid, C., Juarez, A. & Samitier, J., "Dielectrophoresis as a tool to characterize and differentiate isogenic mutants of Escherichia coli," Biophys. J. 91(10), 3937–3945 (2006).
[24] Tang, M., McEwen, G. D., Wu, Y., Miller, C. D. & Zhou, A., "Characterization and analysis of mycobacteria and Gram-negative bacteria and co-culture mixtures by Raman microspectroscopy," FTIR, and atomic force microscopy. Anal. Bioanal. Chem. 405(5), 1577–1591 (2013).
[25] Brennan, P. & Nikaido, H., "The Envelope of Mycobacteria," Annu. Rev. Biochem. 64, 29–63 (1995).
[26] Velayati, A. A. et al., "Differences in cell wall thickness between resistant and nonresistant strains of Mycobacterium tuberculosis: using transmission electron microscopy," Chemotherapy 55(5), 303–307 (2009).
[27] Cheng, I.-F., Chen, T.-Y., Lu, R.-J. & Wu, H.-W., "Rapid identification of bacteria utilizing amplified dielectrophoretic force-assisted nanoparticle-induced surface-enhanced Raman spectroscopy," Nanoscale Res. Lett. 9, 1–8 (2014).
[28] Braschler, T. et al., "Continuous separation of cells by balanced dielectrophoretic forces at multiple frequencies," Lab. Chip 8(2), 280–286 (2008).
[29] Saucedo-Espinosa, M. A. & Lapizco-Encinas, B. H., "Design of insulator-based dielectrophoretic devices: Effect of insulator posts characteristics," J. Chromatogr. A 1422, 325–333 (2015).
[30] Cummings, E. B. & Singh, A. K., "Dielectrophoresis in microchips containing arrays of insulating posts: Theoretical and experimental results," Anal. Chem. 75, 4724–4731 (2003).
[31] Kwon, J.-S., Maeng, J.-S., Chun, M.-S. & Song, S., "Improvement of microchannel geometry subject to electrokinesis and dielectrophoresis using numerical simulations," Microfluid. Nanofluidics 5(1), 23–31 (2008).

[32] Lapizco-Encinas, B. H., Davalos, R. V., Simmons, B. A., Cummings, E. B. & Fintschenko, Y., "An insulator-based (electrodeless) dielectrophoretic concentrator for microbes in water," J. Microbiol. Methods 62(3), 317–326 (2005).
[33] Lapizco-Encinas, B. H., Simmons, B. A., Cummings, E. B. & Fintschenko, Y., "Insulator-based dielectrophoresis for the selective concentration and separation of live bacteria in water," Electrophoresis 25(10-11), 1695–1704 (2004).
[34] Jones, P. V., Staton, S. J. R. & Hayes, M. A., "Blood cell capture in a sawtooth dielectrophoretic microchannel," Anal. Bioanal. Chem. 401(7), 2103–2111 (2011).
[35] Jones, T. B., "Basic theory of dielectrophoresis and electrorotation," IEEE Eng. Med. Biol. Mag. 22(6), 33–42 (2003).
[36] Jones, P. V. et al., "Biophysical separation of Staphylococcus epidermidis strains based on antibiotic resistance," Analyst 140(15), 5152–5161 (2015).
[37] Kang, K. H., Kang, Y. J., Xuan, X. C. & Li, D. Q., "Continuous separation of microparticies by size with direct current-dielectrophoresis," Electrophoresis 27(3), 694–702 (2006).
[38] Barrett, L. M., Skulan, A. J., Singh, A. K., Cummings, E. B. & Fiechtner, G. J., "Dielectrophoretic manipulation of particles and cells using insulating ridges in faceted prism microchannels," Anal. Chem. 77(21), 6798–6804 (2005).
[39] Lewpiriyawong, N., Yang, C. & Lam, Y. C., "Dielectrophoretic manipulation of particles in a modified microfluidic H filter with multi-insulating blocks," Biomicrofluidics 2(3), 034105 (2008).
[40] Chou, C. F. & Zenhausern, F., "Electrodeless dielectrophoresis for micro total analysis systems," IEEE Eng. Med. Biol. Mag. 22(6), 62–67 (2003).
[41] Shafiee, H., Caldwell, J. L., Sano, M. B. & Davalos, R. V., "Contactless dielectrophoresis: a new technique for cell manipulation," Biomed. Microdevices 11(5), 997–1006 (2009).
[42] Elvington, E. S., Salmanzadeh, A., Stremler, M. A. & Davalos, R. V., "Label-free isolation and enrichment of cells through contactless dielectrophoresis," Jove-J. Vis. Exp. (79), e50634 (2013). doi:10.3791/50634
[43] Sano, M. B., Salmanzadeh, A. & Davalos, R. V., "Multilayer contactless dielectrophoresis: Theoretical considerations," Electrophoresis 33(13), 1938–1946 (2012).
[44] Sano, M. B., Caldwell, J. L. & Davalos, R. V., "Modeling and development of a low frequency contactless dielectrophoresis (cDEP) platform to sort cancer cells from dilute whole blood samples," Biosens. Bioelectron. 30(1), 13–20 (2011).
[45] Elitas, M., Martinez-Duarte, R., Dhar, N., McKinney, J. D. & Renaud, P., "Dielectrophoresis-based purification of antibiotic-treated bacterial subpopulations," Lab. Chip 14(11), 1850–1857 (2014).
[46] Martinez-Duarte, R., "Microfabrication technologies in dielectrophoresis applications-A review," Electrophoresis 33(21), 3110–3132 (2012).
[47] Gencoglu, A. et al., "Quantification of pH gradients and implications in insulator-based dielectrophoresis of biomolecules," Electrophoresis 32(18), 2436–2447 (2011).
[48] Kang, Y., Li, D., Kalams, S. A. & Eid, J. E., "DC-Dielectrophoretic separation of biological cells by size," Biomed. Microdevices 10(2), 243–249 (2008).
[49] Chen, Q. et al., "A rapid and low-cost procedure for fabrication of glass microfluidic devices," J. Microelectromechanical Syst. 16(5), 1193–1200 (2007).
[50] Zhang, L. et al., "Fabrication of glass-based microfluidic devices with dry film photoresists as pattern transfer masks for wet etching," Rsc Adv. 5(8), 5638–5646 (2015).
[51] Freitag, A., Vogel, D., Scholz, R. & Dietrich, T. R., "Microfluidic devices made of glass," J. Assoc. Lab. Autom. 6(4), 45–49 (2001).
[52] Gerratt, A. P. & Bergbreiter, S., "Dielectric breakdown of PDMS thin films," J. Micromechanics Microengineering 23(6), 067001 (2013).
[53] Lee, H., Smith, N. J., Pantano, C. G., Furman, E. & Lanagan, M. T., "Dielectric breakdown of thinned BaO–Al2O3–B2O3–SiO2 glass," J. Am. Ceram. Soc. 93(8), 2346–2351 (2010).